Correlation between the decays $h^0 \to \gamma\gamma/gg$ in the MSSM with quark flavour violation

H. Eberl[1], K. Hidaka[2], E. Ginina[1,3]

[1] *Institut für Hochenergiephysik der Österreichischen Akademie der Wissenschaften, A-1050 Vienna, Austria*
[2] *Department of Physics, Tokyo Gakugei University, Koganei, Tokyo 184-8501, Japan*
[3] *VRVis Zentrum für Virtual Reality und Visualisierung Forschungs-GmbH, A-1220 Vienna, Austria*

Abstract

We study the loop-induced decays $h^0 \to \gamma\,\gamma$ and $h^0 \to g\,g$ in the Minimal Supersymmetric Standard Model (MSSM) with quark flavour violation (QFV), identifying h^0 with the Higgs boson with a mass of 125 GeV, where γ and g are photon and gluon, respectively. We perform a MSSM parameter scan and a detailed analysis around a fixed reference point respecting theoretical constraints from vacuum stability conditions and experimental constraints, such as those from B meson data and electroweak precision data, as well as recent limits on supersymmetric (SUSY) particle masses from LHC experiments. We find that (i) the relative deviation of the decay width $\Gamma(h^0 \to g\,g)$ from the Standard Model value, $DEV(g)$, can be large and negative, $\lesssim -15\%$, (ii) the analogous deviation of $\Gamma(h^0 \to \gamma\,\gamma)$ is strongly correlated, $DEV(\gamma) \simeq -1/4\,DEV(g)$ for $DEV(g) \lesssim -4\%$, (iii) the relative deviation of the width ratio $\Gamma(h^0 \to \gamma\,\gamma)/\Gamma(h^0 \to g\,g)$ from the SM value, $DEV(\gamma/g)$, can be large (up to $\sim 20\%$), (iv) the deviations can be large due to the up-type squark loop contributions, (v) the SUSY QFV parameters can have a significant effect on these deviations. Such large deviations can be observed at a future e^+e^- collider like ILC. Observation of the deviation patterns as shown in this study would favour the MSSM with flavour-violating squark mixings and encourage to perform further studies in this model.

1 Introduction

The Standard Model (SM) is a very successful theory of elementary particle physics. It is, however, known to have several essential problems. Primarily it fails to provide an explanation of observed phenomena like the neutrino masses, the matter-antimatter asymmetry, and the dark matter origin. Therefore, it is necessary to search for New Physics, that will help to complete the theory, solve its problems and account the missing details.

Recently a Higgs boson with mass of 125 GeV has been discovered at the Large Hadron Collider (LHC) [1, 2] that behaves like the Higgs boson of the SM. Whether it is indeed the SM Higgs boson or a Higgs boson of New Physics beyond the SM, this is presently one of the most important issues in particle physics. A detailed study of the properties of the Higgs boson can provide a crucial clue in the search for the ultimate New Physics theory. The theory of Supersymmetry (SUSY) is the most prominent candidate for a New Physics theory solving the SM problems. In this paper we study the possibility that the discovered Higgs boson is the lightest CP-even neutral Higgs boson h^0 of the Minimal Supersymmetric Standard Model (MSSM) [3, 4].

In the phenomenological analysis of the MSSM, quark flavour conservation (QFC) is usually assumed, apart from the quark flavour violation (QFV) induced by the Cabibbo-Kobayashi-Maskawa matrix. However, SUSY QFV terms could be present in the mass matrix of the squarks. Especially important can be the mixing terms between the 2nd and the 3rd squark generations, such as $\tilde{c}_{L,R} - \tilde{t}_{L,R}$ mixing terms, where $\tilde{c}$ and $\tilde{t}$ are the charm- and top-squark, respectively.

In [5] we pointed out the importance of the SUSY QFV effects due to squark loop contributions in the decays of the MSSM Higgs boson h^0. We showed that the QFV effect due to $\tilde{c}_{L,R} - \tilde{t}_{L,R}$ mixing can have a major impact on the decay $h^0 \to c\,\bar{c}$, strongly enhancing the deviation of the MSSM Higgs boson decay rate $\Gamma(h^0 \to c\,\bar{c})$ from the SM Higgs boson decay rate $\Gamma(H_{SM} \to c\,\bar{c})$, where c is the charm-quark. In [6] we also showed that the QFV due to $\tilde{c}_{L,R} - \tilde{t}_{L,R}$ mixing can significantly enhance the difference between $\Gamma(h^0 \to b\,\bar{b})$ and $\Gamma(H_{SM} \to b\,\bar{b})$, where b is the bottom-quark.

The loop-induced decays $h^0 \to \gamma\,\gamma$ and $h^0 \to g\,g$ are very sensitive to New Physics since loops of New Physics particles can appear at the lowest order of perturbative expansion of the decay amplitudes. The rates of these loop-induced decays were already calculated including gluonic QCD [7] and electroweak [8] radiative corrections in the SM and also partly in the MSSM with QFC (except [9] mentioned below). In this paper we study the influence of the SUSY QFV due to $\tilde{c}_{L,R} - \tilde{t}_{L,R}$ mixing on $h^0 \to \gamma\,\gamma$ and $h^0 \to g\,g$, including the gluonic two-loop QCD corrections [10]. (We also studied $\tilde{s}_{L,R} - \tilde{b}_{L,R}$ mixing, with $\tilde{s}$ and $\tilde{b}$ the strange- and bottom-squark, respectively, but the effects turned out to be very small.) For this purpose, we perform a MSSM parameter scan respecting theoretical constraints from vacuum stability conditions and experimental constraints, such as those from B meson data and electroweak precision data, as well as recent limits on SUSY particle masses from LHC experiments. In [9] these loop-induced decays were studied in the MSSM with QFV in an effective field theory approach based on dim-6

operators in a so-called κ-framework. However, that paper does not take into account the radiative corrections and the constraints mentioned above, except those from the electroweak precision data. Moreover, it does not include the $\tilde{c}_R - \tilde{t}_R$ mixing effect. As we will point out later, this mixing effect can also play an important role in the considered loop-induced decays.

Although the h^0 decay widths of the $\gamma\gamma$ and gg modes are studied in the SM and the MSSM in many articles [7] - [11], a systematic numerical study of the deviations of the MSSM widths from the SM values taking into account the SUSY QFV effect and the constraints is still missing. In this article we thoroughly perform such a study with special emphasis on the importance of SUSY QFV. Furthermore, we elucidate the sensitivities of measurements at the LHC and at future lepton colliders, such as ILC, to the deviations.

As lepton-flavour violation effect has turned out to be very small in our analysis, we assume lepton flavour conservation. We also assume that the lightest neutralino is the lightest SUSY particle (LSP).

In the following section we introduce the SUSY QFV parameters originating from the squark mass matrices. Details about our parameters scan are given in Section 3. In Section 4 we define the deviations of the widths $h^0 \to \gamma\,\gamma$ and $h^0 \to g\,g$ from the SM and analyse their behaviour in the studied SUSY QFV scenarios. The paper rounds up with conclusions, contained in Section 5, and one short Appendix, where all relevant constraints are listed.

2 Squark mass matrices in the MSSM with flavour violation

In the super-CKM basis of $\tilde{q}_{0\gamma} = (\tilde{q}_{1\mathrm{L}}, \tilde{q}_{2\mathrm{L}}, \tilde{q}_{3\mathrm{L}}, \tilde{q}_{1\mathrm{R}}, \tilde{q}_{2\mathrm{R}}, \tilde{q}_{3\mathrm{R}})$, $\gamma = 1,...6$, with $(q_1, q_2, q_3) = (u, c, t)$, (d, s, b), the up-type and down-type squark mass matrices $\mathcal{M}^2_{\tilde{q}}$, $\tilde{q} = \tilde{u}, \tilde{d}$, at the SUSY scale have the following most general 3×3 block form [12]:

$$\mathcal{M}^2_{\tilde{q}} = \begin{pmatrix} \mathcal{M}^2_{\tilde{q},LL} & \mathcal{M}^2_{\tilde{q},LR} \\ \mathcal{M}^2_{\tilde{q},RL} & \mathcal{M}^2_{\tilde{q},RR} \end{pmatrix}, \quad \tilde{q} = \tilde{u}, \tilde{d}\,. \tag{1}$$

Non-zero off-diagonal terms of the 3×3 blocks $\mathcal{M}^2_{\tilde{q},LL}$, $\mathcal{M}^2_{\tilde{q},RR}$, $\mathcal{M}^2_{\tilde{q},LR}$ and $\mathcal{M}^2_{\tilde{q},RL}$ in Eq. (1) explicitly break the quark-flavour in the squark sector of the MSSM. The left-left and right-right blocks in Eq. (1) are given by

$$\begin{aligned} \mathcal{M}^2_{\tilde{u}(\tilde{d}),LL} &= M^2_{Q_{u(d)}} + D_{\tilde{u}(\tilde{d}),LL}\mathbf{1} + \hat{m}^2_{u(d)}, \\ \mathcal{M}^2_{\tilde{u}(\tilde{d}),RR} &= M^2_{U(D)} + D_{\tilde{u}(\tilde{d}),RR}\mathbf{1} + \hat{m}^2_{u(d)}, \end{aligned} \tag{2}$$

where $M^2_{Q_u} = V_{\mathrm{CKM}} M^2_Q V^\dagger_{\mathrm{CKM}}$, $M^2_{Q_d} \equiv M^2_Q$, $M_{Q,U,D}$ are the hermitian soft SUSY-breaking mass matrices of the squarks, $D_{\tilde{u}(\tilde{d}),LL}$, $D_{\tilde{u}(\tilde{d}),RR}$ are the D-terms, and $\hat{m}_{u(d)}$ are the diagonal mass matrices of the up(down)-type quarks. $M^2_{Q_u}$ is related with $M^2_{Q_d}$ by the CKM

3

matrix V_{CKM} due to the $SU(2)_{\text{L}}$ symmetry. The left-right and right-left blocks of Eq. (1) are given by

$$\mathcal{M}^2_{\tilde{u}(\tilde{d}),RL} = \mathcal{M}^{2\dagger}_{\tilde{u}(\tilde{d}),LR} = \frac{v_2(v_1)}{\sqrt{2}} T_{U(D)} - \mu^* \hat{m}_{u(d)} \cot\beta(\tan\beta), \tag{3}$$

where $T_{U,D}$ are the soft SUSY-breaking trilinear coupling matrices of the up-type and down-type squarks entering the Lagrangian $\mathcal{L}_{int} \supset -(T_{U\alpha\beta}\tilde{u}^\dagger_{R\alpha}\tilde{u}_{L\beta}H^0_2 + T_{D\alpha\beta}\tilde{d}^\dagger_{R\alpha}\tilde{d}_{L\beta}H^0_1)$, μ is the higgsino mass parameter, and $\tan\beta = v_2/v_1$ with $v_{1,2} = \sqrt{2}\langle H^0_{1,2}\rangle$. The squark mass matrices are diagonalized by the 6×6 unitary matrices $U^{\tilde{q}}$, $\tilde{q} = \tilde{u}, \tilde{d}$, such that

$$U^{\tilde{q}}\mathcal{M}^2_{\tilde{q}}(U^{\tilde{q}})^\dagger = \text{diag}(m^2_{\tilde{q}_1}, \ldots, m^2_{\tilde{q}_6}), \tag{4}$$

with $m_{\tilde{q}_1} < \cdots < m_{\tilde{q}_6}$. The physical mass eigenstates $\tilde{q}_i, i = 1, ..., 6$ are given by $\tilde{q}_i = U^{\tilde{q}}_{i\alpha}\tilde{q}_{0\alpha}$.

In this paper we focus on the $\tilde{c}_L - \tilde{t}_L$, $\tilde{c}_R - \tilde{t}_R$, $\tilde{c}_R - \tilde{t}_L$, and $\tilde{c}_L - \tilde{t}_R$ mixing which is described by the QFV parameters M^2_{Q23}, M^2_{U23}, T_{U23} and T_{U32}, respectively. We will also often refer to the QFC parameter T_{U33} which induces the $\tilde{t}_L - \tilde{t}_R$ mixing and plays an important role in this study.

The slepton parameters are defined analogously to the squark ones. All the parameters in this study are assumed to be real, except the CKM matrix V_{CKM}.

3 Parameter scan

We perform a MSSM parameter scan taking into account theoretical constraints from vacuum stability conditions and experimental constraints from K- and B-meson data, the h^0 mass and coupling data and electroweak precision data, as well as limits on SUSY particle masses from recent LHC experiments (see Appendix A). As for the squark generation mixings, we only consider the mixing between the second and third generation of squarks. The mixing between the first and the second generation squarks is very strongly constrained by the K and D meson data [13, 14]. The experimental constraints on the mixing of first and third generation squarks are not so strong [15], but we don't consider this mixing since its effect is essentially similar to that of the mixing of second and third generation squarks. The parameter points are generated by using random numbers in the ranges shown in Table 1, some parameters are fixed (given in the last box). All parameters are defined at scale Q = 1 TeV, except $m_A(pole)$ which is the pole mass of the CP odd Higgs boson A^0. The parameters that are not shown explicitly are taken to be zero. The entire scan lies in the decoupling Higgs limit, i.e. in the scenarios with large $\tan\beta \geq 10$ and large $m_A \geq 800$ GeV (see Table 1), respecting the fact that the discovered Higgs boson is SM-like. It is well known that the lightest MSSM Higgs boson h^0 is SM-like (including its couplings) in this limit. Note that we don't assume the GUT relation for the gaugino masses M_1, M_2, M_3.

The decay widths $\Gamma(h^0 \to \gamma\gamma)_{MSSM}$ and $\Gamma(h^0 \to gg)_{MSSM}$ are calculated with our own code based on the public code SPheno [16, 17]. For the calculation of the MSSM

Table 1: Scanned ranges and fixed values of the MSSM parameters (in units of GeV or GeV^2, except for $\tan\beta$). $M_{1,2,3}$ are the U(1), SU(2), SU(3) gaugino mass parameters.

$\tan\beta$	M_1	M_2	M_3	μ	$m_A(pole)$
$10 \div 30$	$100 \div 2500$	$100 \div 2500$	$2500 \div 5000$	$100 \div 2500$	$800 \div 3000$
M^2_{Q22}	M^2_{Q33}	$|M^2_{Q23}|$	M^2_{U22}	M^2_{U33}	$|M^2_{U23}|$
$2500^2 \div 4000^2$	$2500^2 \div 4000^2$	$< 1000^2$	$1000^2 \div 4000^2$	$600^2 \div 3000^2$	$< 1200^2$
M^2_{D22}	M^2_{D33}	$|M^2_{D23}|$	$|T_{U23}|$	$|T_{U32}|$	$|T_{U33}|$
$2500^2 \div 4000^2$	$1000^2 \div 3000^2$	$< 1000^2$	< 4000	< 4000	< 4000
$|T_{D23}|$	$|T_{D32}|$	$|T_{D33}|$	$|T_{E33}|$		
< 1000	< 1000	< 1000	< 500		

M^2_{Q11}	M^2_{U11}	M^2_{D11}	M^2_{L11}	M^2_{L22}	M^2_{L33}	M^2_{E11}	M^2_{E22}	M^2_{E33}
4500^2	4500^2	4500^2	1500^2	1500^2	1500^2	1500^2	1500^2	1500^2

spectrum we use the version `SPheno-v3.3.8`. The computation includes lowest order 1-loop contributions and gluonic 2-loop QCD corrections (i.e. NLO QCD corrections) to quark loops [10] [1]. The lowest order 1-loop contributions to $\Gamma(h^0 \to \gamma\gamma)_{MSSM}$ stem from the loops with SM particles, quarks (t, b, ...), charged leptons (τ^-, ...) and $W^\pm$ boson and SUSY particles, squarks ($\tilde{u}$, $\tilde{d}$), charged sleptons ($\tilde{\tau}^-$, ...), charginos $\tilde{\chi}^\pm$ and charged Higgs bosons $H^\pm$. The lowest order 1-loop contributions to $\Gamma(h^0 \to gg)_{MSSM}$ stem from the loops with quarks (t, b, ...) and squarks ($\tilde{u}$, $\tilde{d}$). In order to stay consistent we also use our own code for the SM decay widths $\Gamma(h^0 \to \gamma\gamma)_{SM} \equiv \Gamma(H_{SM} \to \gamma\gamma)$, and $\Gamma(h^0 \to gg)_{SM} \equiv \Gamma(H_{SM} \to gg)$ including the gluonic 2-loop QCD corrections [10]. We have cross-checked them numerically with the decoupling limit of the MSSM results. The Higgs mass in the kinematic factors of the widths is fixed by the measured mass at LHC, $m_{h^0} = 125.09$ GeV to avoid an artificially large dependence stemming from the kinematic factor in $\Gamma(h^0 \to \gamma\gamma/gg)_{MSSM}$, which is proportional to $m_{h^0}^3$. All MSSM input parameters are taken as $\overline{\text{DR}}$ parameters at the scale $Q = 1$ TeV and then transformed by RGEs to those at the scale of $Q = m_{h^0} = 125.09$ GeV. The masses and rotation matrices

---

[1] The gluonic 2-loop QCD corrections to the squark loops are negligibly small since the squark-loop contributions to the widths are rather small due to large squark masses from the LHC limit (see Appendix A). As the corrections to small contributions are very small, we can neglect such corrections. We can also neglect SUSY-QCD corrections to the quark/squark-loops since gluino/squarks are required to be so heavy by the LHC limits (see Appendix A) that gluino/squark-loop corrections (i.e. SUSY-QCD corrections) to the widths are very small. Moreover, the NNLO QCD corrections [7] and the NLO electroweak (EW) corrections [8] to the widths are found to be much smaller than the NLO QCD corrections. Therefore, we take into account only the gluonic 2-loop QCD corrections (i.e. NLO QCD corrections) to quark-loop contributions to $\Gamma(h^0 \to \gamma\gamma/gg)_{MSSM}$.

of the sfermions are renormalized at one-loop level within SPheno based on the technique given in [18].

From 2850000 input points generated in the scan about 285500 survived all constraints. These are about 10%. We show these survival points in all scatter plots in this article.

4 Deviation of the MSSM widths from the SM

We define the relative deviation of the MSSM width from the SM width as[2]

$$DEV(X) = \Gamma(h^0 \to XX)_{MSSM}/\Gamma(h^0 \to XX)_{SM} - 1 \,, \text{ with } X = \gamma, g \,, \tag{5}$$

where we identify h^0 with the Higgs boson with a mass of 125.09 GeV.
The relative deviation of the width ratio from the SM prediction is defined as

$$DEV(\gamma/g) = [\Gamma(\gamma)/\Gamma(g)]_{MSSM}/[\Gamma(\gamma)/\Gamma(g)]_{SM} - 1 \tag{6}$$

with

$$\Gamma(X) = \Gamma(h^0 \to XX), \text{where } X = \gamma, g. \tag{7}$$

Note that $DEV(\gamma/g)$ in Eq. (6) can be written also directly in terms of $DEV(\gamma)$ and $DEV(g)$,

$$DEV(\gamma/g) = \frac{DEV(\gamma) + 1}{DEV(g) + 1} - 1 \,. \tag{8}$$

Before we show the results of the full parameter scan, we briefly comment on an expected qualitative behaviour of $DEV(g)$. One can approximate $DEV(g)$ in an effective field theory approach based on dim-6 operators parametrized in a so-called κ-framework [9], assuming that the SM contribution stems only from the top-loop and neglecting the Higgs mass in the amplitude. Based on the result for $\delta\kappa_g$ given in [9], we can write the approximation for $DEV(g) \sim 2\delta\kappa_g = DEV(g)^{approx}$ in our convention (see Section 2),

$$DEV(g)^{approx} = \frac{v^2}{4} \left[\frac{1}{m_{\tilde{t}_L}^2} \left(y_t^2 - \frac{|T_{U23}|^2}{m_{\tilde{c}_R}^2} \right) + \frac{1}{m_{\tilde{t}_R}^2} \left(y_t^2 - \frac{|T_{U32}|^2}{m_{\tilde{c}_L}^2} \right) - \frac{|T_{U33}|^2}{m_{\tilde{t}_L}^2 \, m_{\tilde{t}_R}^2} \right], \tag{9}$$

where $y_t = \sqrt{2}\, m_t/v_2 = g\, m_t/(\sqrt{2}\, m_W \sin\beta)$ is the top-quark Yukawa coupling, $v = \sqrt{v_1^2 + v_2^2} = 2\, m_W/g = 242$ GeV is the vacuum expectation value, m_t is the top-quark mass, m_W is the W-boson mass, and g is the SU(2) gauge coupling constant. In Eq. (9) we have neglected terms $\propto \mu/\tan\beta$ because we use in this numerical study large values of $\tan\beta$ (≥ 10), see Eq. (3). Note that Eq. (9) is not a function of M_{U23}^2 and M_{Q23}^2. The

---

[2]For reference, the SM predictions (at 68% CL) of [19] are $\Gamma(\gamma)_{SM} = (1.08^{+0.03}_{-0.02}) \cdot 10^{-5}$ GeV and $\Gamma(g)_{SM} = (3.61 \pm 0.06) \cdot 10^{-4}$ GeV, and those of [20] are $\Gamma(\gamma)_{SM} = (9.31 \pm 0.09) \cdot 10^{-6}$ GeV and $\Gamma(g)_{SM} = (3.35 \pm 0.21) \cdot 10^{-4}$ GeV.
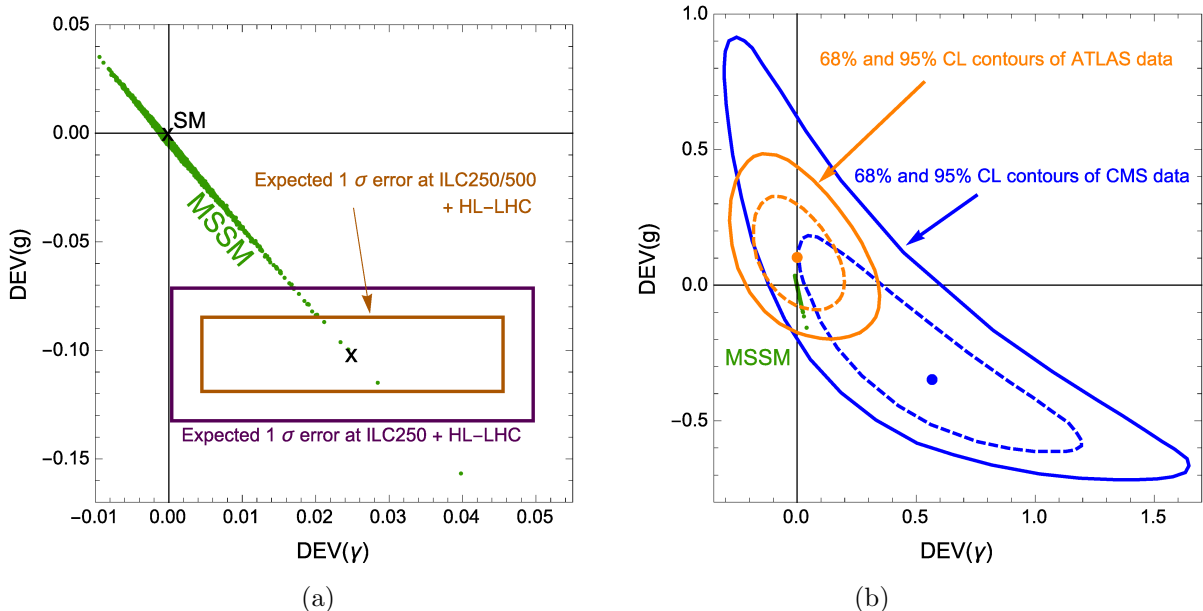
Figure 1: The scatter plot of the scanned parameter points within the ranges given in Table 1 in the $DEV(\gamma)$ - $DEV(g)$ plane. (a): The expected 1σ errors at ILC250/500 + HL-LHC [ILC250 + HL-LHC]; the black cross at $(DEV(\gamma), DEV(g))=(0.025, -0.102)$ shows a possibly measured point of Eq. (11) and the orange and purple boxes indicate expected 1σ errors of Eqs. (15) and (16), respectively. (b): The 68% and 95% CL contours of the recent ATLAS/CMS data [23, 24].

terms $m^2_{\tilde{c}_{L,R}}$ and $m^2_{\tilde{t}_{L,R}}$ are diagonal entries of the mass matrix $\mathcal{M}^2_{\tilde{q}}$, Eq. (1). For values much larger than v we can approximate them by $m^2_{\tilde{c}_L} \simeq M^2_{Q22}$, $m^2_{\tilde{c}_R} \simeq M^2_{U22}$, $m^2_{\tilde{t}_L} \simeq M^2_{Q33}$, and $m^2_{\tilde{t}_R} \simeq M^2_{U33}$.

From Eq. (9) we see that $DEV(g)^{approx}$ depends only on the squared absolute values of T_{U23}, T_{U32}, and T_{U33}. When all these three parameters go to zero, $DEV(g)^{approx}$ is small and positive. For large values of $|T_{U23}|, |T_{U32}|$, and $|T_{U33}|$ $DEV(g)^{approx}$ becomes large and negative. Furthermore, $DEV(g)^{approx}$ also grows when $m^2_{\tilde{c}_{L,R}}$ and/or $m^2_{\tilde{t}_{L,R}}$ decrease.

In the following we show the results of a full parameter scan without using this effective field theory approximation.

In Fig. 1 we show the scatter plot of the scanned parameter points within the ranges given in Table 1 in the $DEV(\gamma) - DEV(g)$ plane. We see that $DEV(g)$ is mostly negative and goes down to more than -10%, and that there is a strong correlation between $DEV(\gamma)$ and $DEV(g)$,

$$DEV(\gamma) \simeq -\frac{1}{4}DEV(g). \tag{10}$$

Thus we also have $DEV(\gamma)^{approx} \simeq -\frac{1}{4}DEV(g)^{approx}$. This feature is due to the fact that the amplitude for $h^0 \to \gamma\gamma$ is dominated by the W-boson loop contribution. The second

important contribution to $h^0 \to \gamma\gamma$ stems from the top-quark loop. The decay $h^0 \to gg$ is dominated by the top-quark loop contribution. In the scenarios we are interested in, the up-type squark loop contributions to $h^0 \to \gamma\gamma/gg$ can be large. All other SUSY contributions are relatively small, giving together less than 0.5% in our study. Hence both $DEV(\gamma)$ and $DEV(g)$ are dominated by the same common source (i.e. $\tilde{u}_{1,2}$-loops) which together with the W-loop dominance leads to the strong correlation.

Qualitatively our results are consistent with $DEV(g)^{approx}$ and $DEV(\gamma)^{approx}$ but it is hard to compare directly numerically because of the different usage of the MSSM input parameters, see the description at the end of Section 3.
The large deviations shown in Fig. 1 can be experimentally observed at a future e^+e^- collider such as ILC [21] and/or CLIC [22]. The abbreviations "ILC250/500 + HL-LHC" and "ILC250 + HL-LHC" are explained below. In Fig. 1(b) the recent LHC data of the coupling modifiers (κ_γ, κ_g) transformed into the ($DEV(\gamma), DEV(g)$) plane by using the relation $DEV(X) = \kappa_X^2 - 1$ are shown, where $\kappa_X = C(h^0XX)/C(h^0XX)_{SM}$ with $C(h^0XX)$ being the coupling of h^0XX. It is seen that the errors of the LHC data are very large and both the SM and the MSSM are allowed by the ATLAS/CMS data on the h^0 couplings $C(h^0\gamma\gamma)$ and $C(h^0gg)$.
If the measured point at ILC + HL-LHC was around ($DEV(\gamma), DEV(g)$) = (0.025, -0.10) as shown in Fig. 1(a), then the data would disfavour the SM and favour the MSSM. If the measured point was around ($DEV(\gamma), DEV(g)$) = (-0.05, -0.10), then we could say that the data disfavours both the SM and the MSSM.

In Fig. 2 we show the scatter plots of the scanned parameter points within the ranges given in Table 1 in the T_{U33} - DEV(γ) (a), T_{U33} - DEV(g) (b), and T_{U33} - DEV(γ/g) (c) planes. We see that DEV(g) and DEV(γ/g) can be large in the scanned parameter ranges for large values of $|T_{U33}|$. This means that the $\tilde{u}_{1,2}$-loop ($\sim$ stop/scharm loops) contributions to these loop-induced decays are quite important. As in Figure 1 the deviations shown can be observed at a future e^+e^- collider (ILC/CLIC).
In all three plots of Fig. 2 we see the parabolic increase of the DEV's for increasing $|T_{U33}|$ as this is discussed after Eq. (9). The less populated region around $T_{U33} = 3$ TeV stems from the fact that the upper limit of the m_{h^0} constraint is often violated there.

In order to show the importance of the QFV effect, in Fig. 3 we show the scatter plot in the $T_{U32} - DEV(\gamma)$ (a), $T_{U32} - DEV(g)$ (b), and $T_{U32} - DEV(\gamma/g)$ (c) planes. In Fig. 3 we have a similar pattern as before in Fig. 2 but with the maximal results at slightly smaller values of the dependent variable, $|T_{U32}| \sim 2.5$ TeV. Again the parabolic shape is seen. And we see that in order to have large results we need the absolute value of both, the QFC parameter T_{U33} and the QFV parameter T_{U32}, large.

We have obtained a similar dependence on T_{U23} to that on T_{U32}. Hence we do not show here the analogous plots on T_{U23}. In the parameter scan the average value of M_{U22}^2 is 1.8 times larger than that of M_{U33}^2. Therefore, the prefactor of $|T_{U23}|^2$ in Eq. (9) is 1.8 times smaller in average than that of $|T_{U32}|^2$ leading to somewhat milder $|T_{U23}|^2$ dependence of the deviations than that of $|T_{U32}|^2$. However, this choice of different mass ranges is just for a good efficiency (a good survival probability) of parameter scan in search for large deviations. The deviations can be enhanced by relatively light stop/scharm masses (see
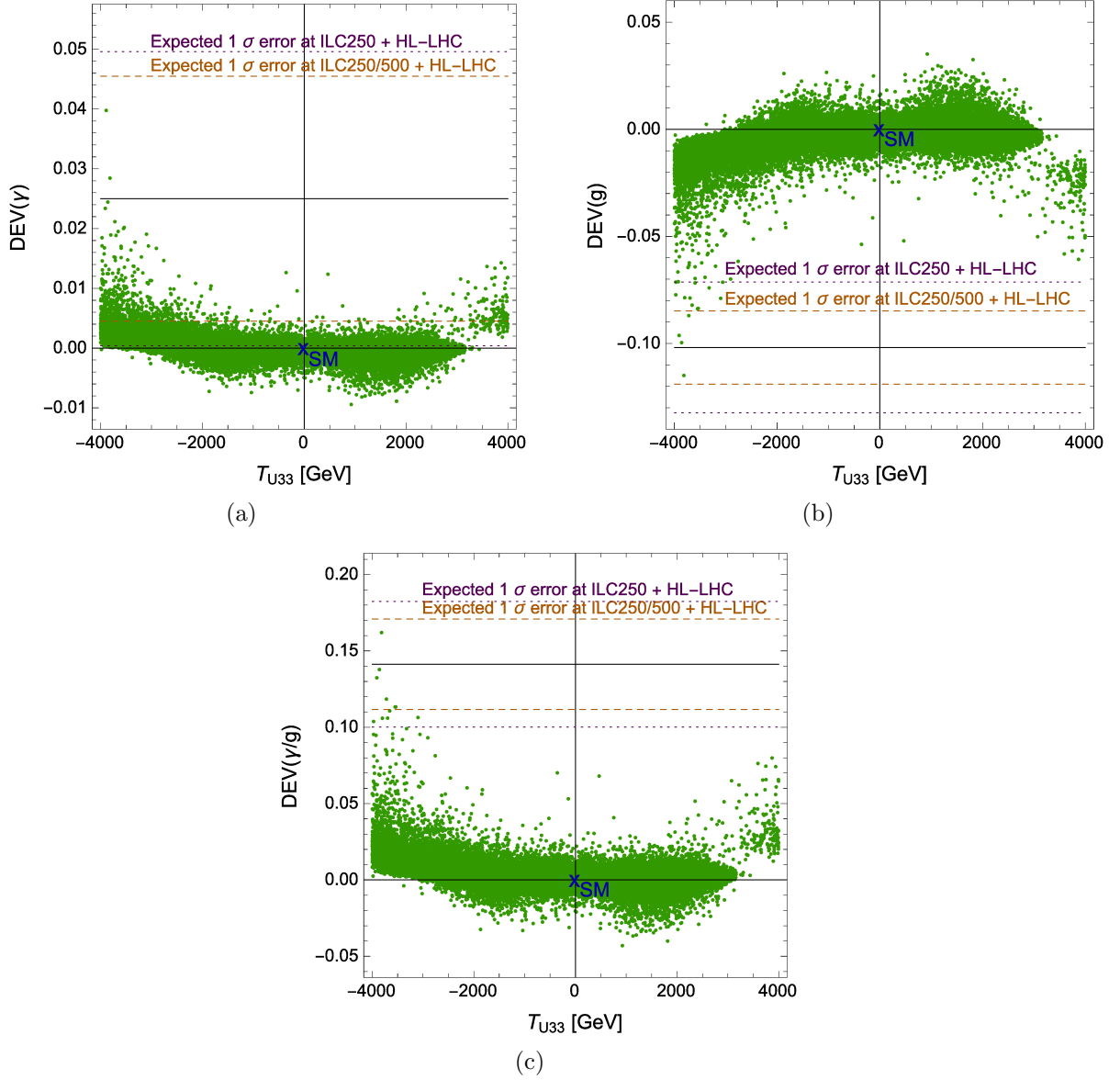
8

Figure 2: The scatter plots of the scanned parameter points within the ranges given in Table 1 in (a): T_{U33} - DEV(γ); (b): T_{U33} - DEV(g); (c): T_{U33} - DEV(γ/g) planes. The expected 1σ errors at ILC250/500 + HL–LHC [ILC250 + HL–LHC] are also shown. The black horizontal solid lines at (DEV(γ), DEV(g), DEV(γ/g))=(0.025, -0.102, 0.141) show possibly measured values of Eq. (11) and the orange and purple dashed-lines indicate expected 1σ errors of Eqs. (15) and (16), respectively.

Eq. (9)). Hence, relatively light mass ranges are taken for M_{U22}^2 and M_{U33}^2 in Table 1. In order to confirm that this choice does not affect our final conclusion essentially, we have performed the same parameter scan by taking common mass ranges [(0.6 TeV)^2, (4.0 TeV)^2] for $\{M_{Q22}^2, M_{Q33}^2, M_{U22}^2, M_{U33}^2, M_{D22}^2, M_{D33}^2\}$. We have obtained very similar scan

results with slightly enhanced T_{U23} dependence and much smaller survival probability of the scan.

The common feature of the scan results is that the DEV's are significantly enhanced by the large values of the trilinear couplings $T_{U23}, T_{U32}, T_{U33}$. This can be explained as follows:

- The $\tilde{c}_{R/L} - \tilde{t}_{R/L}$ mixings can be large for large QFV parameters $M_{Q23}^2, M_{U23}^2, T_{U23}$, and T_{U32}, for which the lighter up-type squarks $\tilde{u}_{1,2}$ can be strong mixtures of $\tilde{c}_{R/L} - \tilde{t}_{R/L}$.

- In our decoupling Higgs scenario (with large m_A and large $\tan\beta$), $h^0 \simeq \mathrm{Re}(H_2^0)$ and hence $(T_{U23}, T_{U32}, T_{U33}) \simeq (h^0\tilde{t}_L\tilde{c}_R, h^0\tilde{t}_R\tilde{c}_L, h^0\tilde{t}_L\tilde{t}_R)$ couplings.

Thus, the $h^0\tilde{u}_{1,2}\tilde{u}_{1,2}$ couplings and therefore also the $\tilde{u}_{1,2}$-loop contributions to $\Gamma(h^0 \to \gamma\gamma, gg)$ can be enhanced by large $T_{U23}, T_{U32}, T_{U33}$, which results in the significant correlations between $T_{U23}, T_{U32}, T_{U33}$, and $DEV(\gamma), DEV(g), DEV(\gamma/g)$. This explains the appearance of these T_U's in Eq. (9).

Our analysis has shown that the correlations between the deviations $DEV(\gamma)$, $DEV(g)$, $DEV(\gamma/g)$ and all the FV/FC parameters other than those from the $\tilde{u}$ sector, such as $T_{U23}, T_{U32}, T_{U33}$ and the stop/scharm masses, are very weak (see Eq.(9)). This means that the deviations $DEV(\gamma)$, $DEV(g)$, $DEV(\gamma/g)$ are quite insensitive to the parameters other than those of the up-type squark sector. The latter is due to the fact that in our decoupling Higgs scenario $h^0 \simeq \mathrm{Re}(H_2^0)$. Hence, the contributions of the down-type squark loops and the charged slepton loops to the decay widths $\Gamma(h^0 \to \gamma\gamma)$ and $\Gamma(h^0 \to gg)$ are very small. Note that H_2^0 couples to $\tilde{t}_L/\tilde{c}_L$ - $\tilde{t}_R/\tilde{c}_R$ but does not to $\tilde{b}_L/\tilde{s}_L$ - $\tilde{b}_R/\tilde{s}_R$. Furthermore, for $DEV(\gamma)$, the charged Higgs and the chargino contributions always remain in the few-per mille range.

It is important to discuss the expected experimental errors. We use two supposed data sets, data set A: ILC250/500 + HL-LHC and for collecting data without having a 500 GeV ILC, data set B: ILC250 + HL-LHC. The explanation of what "ILC250 + HL-LHC" and "ILC250/500 + HL-LHC" stand for is given in detail in the caption of Table 1 of [21], named there "ILC250" and "ILC500". In order to discuss the experimental and theoretical errors we fix a possibly measured point,

$$\{DEV(\gamma)_c, DEV(g)_c, DEV(\gamma/g)_c\} = \{2.5\%, -10.2\%, 14.1\%\}. \tag{11}$$

This point is shown in Fig. 1(a) by a black cross and in the Figs. 2-3 by solid horizontal lines. We use the relative estimated experimental 1σ errors on the couplings $h\gamma\gamma$ and hgg and their ratio in the EFT fit framework,

$$\text{dataset A}: \quad \{\delta^r g_\gamma, \delta^r g_g, \delta^r g_{\gamma/g}\} = \{1\%, 0.95\%, 1.3\%\}, \tag{12}$$

$$\text{dataset B}: \quad \{\delta^r g_\gamma, \delta^r g_g, \delta^r g_{\gamma/g}\} = \{1.2\%, 1.7\%, 1.8\%\}, \tag{13}$$

where $\delta^r y$ is defined as the relative error $\Delta y/y$ of the parameter y. The values for $\delta^r g_\gamma$ and $\delta^r g_g$ are taken from Table 1 in [21] and the value for $\delta^r g_{\gamma/g}$ we got from [25] using the same EFT fit program as in [21]. Using

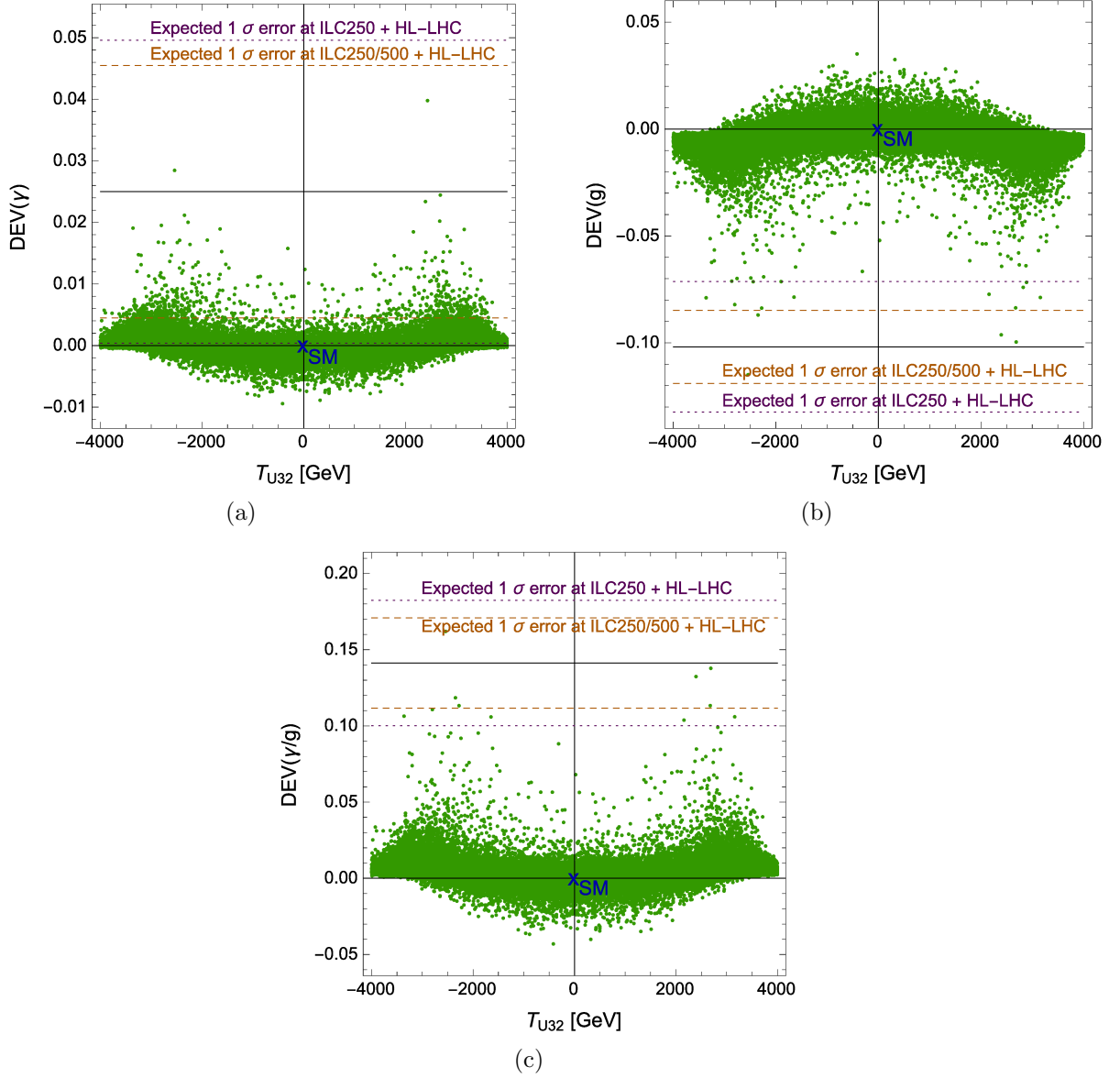$$\Delta DEV(X) = 2(DEV(X)_c + 1)\delta^r g_X, \quad X = \gamma, g, \gamma/g, \tag{14}$$

10

(a)

(b)

(c)

Figure 3:   The scatter plot in the T_{U32} - DEV(γ) (a), T_{U32} - DEV(g) (b), and T_{U32} - DEV(γ/g) (c) planes. The expected 1σ errors at ILC250/500 + HL-LHC [ILC250 + HL-LHC] are also shown as in Fig. 2.

we get the 1σ errors for our DEV's,

$$\text{dataset A}:\quad \{\Delta DEV(\gamma), \Delta DEV(g), \Delta DEV(\gamma/g)\} = \{2.1\%, 1.7\%, 3.0\%\}, \quad (15)$$

$$\text{dataset B}:\quad \{\Delta DEV(\gamma), \Delta DEV(g), \Delta DEV(\gamma/g)\} = \{2.5\%, 3.1\%, 4.1\%\}. \quad (16)$$

The 1σ error bands are $DEV(X)_c \pm \Delta DEV(X)$, shown by boxes in Fig 1a and by dashed and dotted lines in Fig. 2 and Fig. 3.

11

In all three figures Figs. 1-3 we see that there are only a few dozens of points where we have really a large deviation from the SM expectation values. This is just a matter of statistics because we perform a scan in a 22-dimensional parameter space. Thus we choose a reference scenario where we have large DEV's and then variate the most interesting parameters around this point P1. All MSSM input parameters for P1 are shown in Table 2 giving the DEV's in Eq. (11).

This scenario P1 satisfies all present experimental and theoretical constraints, see Appendix A. The resulting physical masses of the particles are shown in Table 3. For the calculation of the masses and the mixing, as well as for the low-energy observables, especially those in the B and K meson sectors (see Table 4), we use the public code SPheno v3.3.8 [16, 17]. For the calculation of the coupling modifier $\kappa_b = C(h^0 b\bar{b})/C(h^0 b\bar{b})_{SM}$ (or equivalently the deviation $DEV(b)(= \kappa_b^2 - 1)$ of the width $\Gamma(h^0 \to b\bar{b})$ from its SM value) we compute the width $\Gamma(h^0 \to b\bar{b})$ at full one-loop level in the MSSM with QFV by using the code developed by us [6]. We obtain $\kappa_b = 0.927$ (or $DEV(b) = -0.141$) which satisfies the LHC data in Table 4. For the B and K meson observables we get; $B(b \to s\gamma) = 3.177 \cdot 10^{-4}$, $B(b \to s\ l^+l^-) = 1.588 \cdot 10^{-6}$, $B(B_s \to \mu^+\mu^-) = 3.065 \cdot 10^{-9}$, $B(B^+ \to \tau^+\nu) = 9.956 \cdot 10^{-5}$, $\Delta M_{B_s} = 19.606[ps^{-1}]$, $|\epsilon_K| = 2.205 \cdot 10^{-3}$, $\Delta M_K = 2.322 \cdot 10^{-15}\ (GeV)$, $B(K_L^0 \to \pi^0\nu\bar{\nu}) = 2.307 \cdot 10^{-11}$, and $B(K^+ \to \pi^+\nu\bar{\nu}) = 7.734 \cdot 10^{-11}$, all of which satisfy the constraints of Table 4.

Table 2: The MSSM parameters for the reference point P1 (in units of GeV or GeV^2 expect for $\tan\beta$)

$\tan\beta$	M_1	M_2	M_3	μ	$m_A(pole)$
16	1270	500	4800	1260	1960

M^2_{Q22}	M^2_{Q33}	M^2_{Q23}	M^2_{U22}	M^2_{U33}	M^2_{U23}
3660^2	2520^2	550^2	3710^2	1435^2	875^2

M^2_{D22}	M^2_{D33}	M^2_{D23}	T_{U23}	T_{U32}	T_{U33}
3620^2	2720^2	925^2	760	1560	- 4200

T_{D23}	T_{D32}	T_{D33}	T_{E33}
-565	690	270	- 470

M^2_{Q11}	M^2_{U11}	M^2_{D11}	M^2_{L11}	M^2_{L22}	M^2_{L33}	M^2_{E11}	M^2_{E22}	M^2_{E33}
4500^2	4500^2	4500^2	1500^2	1500^2	1500^2	1500^2	1500^2	1500^2

In Fig. 4 we show the contour plots of DEV(γ/g) in the QFV/QFC parameter plane around P1. The reference point is marked by a green "x". We see that $DEV(\gamma/g)$ is really large in a large region of the parameter planes and that the effect of the QFV parameters $M^2_{U23}, T_{U23}, T_{U32}$ (and the QFC parameter T_{U33} also) on the $DEV(\gamma/g)$ is very important.

Table 3: Physical masses in GeV of the particles for the scenario of Table 2.

$m_{\tilde{\chi}_1^0}$	$m_{\tilde{\chi}_2^0}$	$m_{\tilde{\chi}_3^0}$	$m_{\tilde{\chi}_4^0}$	$m_{\tilde{\chi}_1^+}$	$m_{\tilde{\chi}_2^+}$
532.1	1242	1271	1310	532.3	1275

m_{h^0}	m_{H^0}	m_{A^0}	m_{H^+}
125.5	1960	1960	1962

$m_{\tilde{g}}$	$m_{\tilde{u}_1}$	$m_{\tilde{u}_2}$	$m_{\tilde{u}_3}$	$m_{\tilde{u}_4}$	$m_{\tilde{u}_5}$	$m_{\tilde{u}_6}$
4562	725	2204	3497	3551	4380	4386

$m_{\tilde{d}_1}$	$m_{\tilde{d}_2}$	$m_{\tilde{d}_3}$	$m_{\tilde{d}_4}$	$m_{\tilde{d}_5}$	$m_{\tilde{d}_6}$
2173	2421	3467	3497	4380	4386

We again see the parabolic behaviour on all the T_U parameters. For this parameter point the dependence on T_{U32} and T_{U23} is of similar size and the dependence on T_{U33} varies from -3% up to 16% in the allowed region. Fig. 4(c) shows a strong dependence on $\tilde{c}_R - \tilde{t}_R$ mixing parameter M_{U23}^2 which means that for large M_{U23}^2 the "linearized" approximation Eq. (9) is not good anymore. There one should add higher orders to Eq. (9) which includes M_{U23}^2.

Finally, we also discuss the theoretical errors. The theoretical uncertainties of the MSSM predictions are twofold. If we consider a fixed MSSM parameter point, the total theoretical error can be split into two parts: one is the uncertainty due to unknown (higher order) loop contributions and the other one - the uncertainty due to errors of the SM input parameters. The former uncertainty we call scale uncertainty and the latter one - parametric uncertainty. The scale uncertainty can be estimated by varying the renormalization scale Q from $Q = m_{h^0}/2$ up to $Q = 2m_{h^0}$.

We can write the relative parametric uncertainty as

$$\delta^{r,P}DEV(X) = \left| \frac{m_t}{DEV(X)} \frac{\partial DEV(X)}{\partial m_t} \right| \delta^r m_t \oplus \left| \frac{\alpha_s}{DEV(X)} \frac{\partial DEV(X)}{\partial \alpha_s} \right| \delta^r \alpha_s \,, \qquad (17)$$

with $X = \gamma, g, \gamma/g$. We have found that we can neglect the parametric uncertainties due to all the other SM parameters such as m_b, α_{EM}, m_Z etc.. We use as input the on-shell top-mass, $m_t = 173$ GeV with $\delta^r m_t = 0.23\%$, and $\alpha_s \equiv \alpha_s(m_Z)_{\overline{MS}} = 0.1181$ with $\delta^r \alpha_s = 0.93\%$ [52]. We get for the reference point P1 at 1σ

$$
\begin{aligned}
\delta^{r,P}DEV(\gamma) &= |-1.7|\delta^r m_t \oplus |3.0|\delta^r \alpha_s = 0.4\% \oplus 2.8\% \,, \\
\delta^{r,P}DEV(g) &= |-0.2|\delta^r m_t \oplus |2.8|\delta^r \alpha_s = 0.05\% \oplus 2.6\% \,, \\
\delta^{r,P}DEV(\gamma/g) &= |-0.5|\delta^r m_t \oplus |3.1|\delta^r \alpha_s = 0.1\% \oplus 2.9\% \,.
\end{aligned}
$$

One would guess that for $DEV(\gamma)$ there should be a small coefficient in front of $\delta^r \alpha_s$. This is not the case because α_s has a strong influence on the calculation of the running top
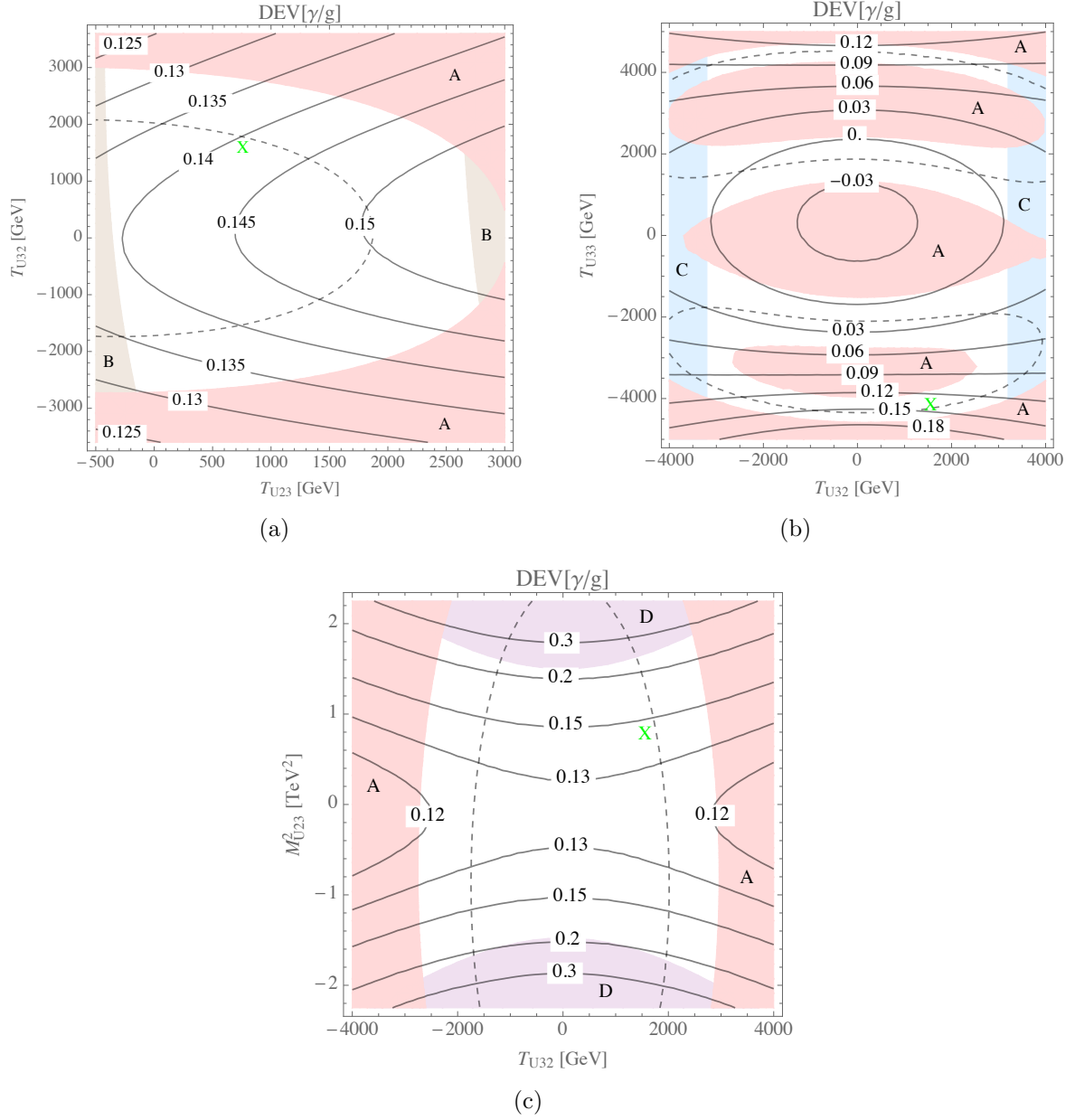
Figure 4: Contour plots of DEV(γ/g) in the T_{U32} - T_{U23} (a), T_{U32} - T_{U33} (b), T_{U32} - M_{U23}^2 (c) planes. The parameters other than the shown ones in each plane are fixed as in Table 2. The "X" marks P1 in the plots. The shown forbidden areas are due to the constraints: $A \equiv m_{h^0}$, $B \equiv \mathrm{B}(B_s \to \mu^+\mu^-)$, $C \equiv$ vacuum stability condition, $D \equiv m_{\tilde{u}_1}$. The dashed lines are the contours of $m_{h^0} = 125.09$ GeV.

Yukawa coupling at $Q = m_{h^0}$ and on that of the $\tilde{u}$ parameters entering the $h^0\tilde{u}\tilde{u}^*$ couplings.

From the scale variation we get

$$\delta^{r,Q}DEV(\gamma) = \begin{matrix} 2.3\% \\ -2.1\% \end{matrix} \simeq 2.3\%,$$

$$\delta^{r,Q}DEV(g) = \begin{matrix} 2.9\% \\ -2.6\% \end{matrix} \simeq 2.9\%,$$

$$\delta^{r,Q}DEV(\gamma/g) = \begin{matrix} 3.2\% \\ -2.8\% \end{matrix} \simeq 3.2\%.$$

The upper value is for $Q = m_{h^0}/2$ and the lower one for $Q = 2m_{h^0}$. Thus we estimate the total theoretical relative and absolute errors $\Delta DEV(X) = \delta^r DEV(X) DEV(X)_c$, at 1σ for the point P1,

$$\delta^r DEV(\gamma) = 5.1\%, \quad \Delta DEV(\gamma) = 0.13\%,$$
$$\delta^r DEV(g) = 5.5\%, \quad \Delta DEV(g) = 0.55\%,$$
$$\delta^r DEV(\gamma/g) = 6.1\%, \quad \Delta DEV(\gamma/g) = 0.85\%,$$

where the parametric uncertainties are added quadratically and the scale uncertainty is added to them linearly. Comparing this result with Eqs. (15) and (16) we see that the theoretical errors are one order smaller than the experimental ones at P1. From Eqs. (11), (15), (16) and the theoretical errors, we see that ILC cannot miss this SUSY signal in case the scenario P1 (or similar ones) is realized in Nature.

Using the LO (lowest order) results instead of the NLO results at P1, the relative shifts of the DEV's are found to be very small (less than 1%). This is due to the fact that in our computation the NLO QCD corrections are included only in the SM parts which dominate the MSSM widths.

One might think that the experimental and theoretical improvement expected in the low-energy observables could exclude the flavour-violating squark scenarios in the first place, way before the beginning of the HL-LHC or the ILC. On the other hand, the low-energy observables have both experimental and theoretical errors and currently the latter errors tend to be comparable to (or larger than) the former ones as shown in Table 4. The theoretical improvement expected in the low-energy observables is rather unclear. Only if the observed values with almost zero errors perfectly agree with the SM predictions with almost zero errors, the possibility of the flavour-violating squark scenarios will be excluded.

5 Conclusions

We have studied the correlation between the loop-induced decays $h^0 \to \gamma\gamma$ and $h^0 \to gg$ in the MSSM with QFV. From a full parameter scan and a detailed analysis around a fixed reference point, respecting all the relevant theoretical and experimental constraints, we have found that

- the relative deviation of the MSSM decay width $\Gamma(h^0 \to g\,g)$ from the Standard Model value, $DEV(g)$, can be large and negative down to $\sim$ -15% in the studied parameter ranges,

- there is a strong correlation between $DEV(\gamma)$ and $DEV(g)$,

- the relative deviation of the width ratio $DEV(\gamma/g)$ from the SM value can be large (up to $\sim$ 20%) in the studied parameter ranges,

- both SUSY QFV and QFC up-type squark parameters can have a strong influence on these deviations and their contributions add up.

Such large deviations can be observed at a future e^+e^- collider such as ILC and CLIC. Observation of the deviation patterns as shown in this study would favour the MSSM with flavour-violating squark mixings and encourage to perform further studies in this model.

Acknowledgments

A   Theoretical and experimental constraints

The experimental and theoretical constraints taken into account in the present work are discussed in detail in [26]. Here we only list the updated constraints from K- and B-physics and those on the Higgs boson mass and coupling in Table 4.

The h^0 couplings that receive SUSY QFV effects significantly are $C(hbb)$ [6], $C(hcc)$ [5], $C(hgg)$ and $C(h\gamma\gamma)$ [3]. The measurement of $C(hcc)$ is very difficult due to huge QCD backgrounds at LHC; there is no significant experimental data on $C(hcc)$ at this moment. Hence, the relevant h couplings to be compared with the LHC observations are $C(hbb)$, $C(hgg)$ and $C(h\gamma\gamma)$. The MSSM predictions for the couplings $C(hgg)$ and $C(h\gamma\gamma)$ are allowed by the current LHC data as shown in Fig. 1(b). Therefore, we list the LHC data on $C(hbb)$ (κ_b) in Table 4.

In [15] the QFV decays $t \to qh$ with $q = u, c$, have been studied in the general MSSM with QFV. It is found that these decays cannot be visible at the current and high luminosity LHC runs due to the very small decay branching ratios B($t \to qh$).

---

[3] Precisely speaking, in principle, $C(htt)$ coupling could also receive SUSY QFV effects significantly. However, predicting the (effective) coupling $C(htt)$ at loop levels in the MSSM is very difficult since its theoretical definition in the context of tth production at LHC is unclear [27].

In addition to these we also require our scenarios to be consistent with the following updated experimental constraints:

Table 4: Constraints on the MSSM parameters from the K- and B-meson data relevant mainly for the mixing between the second and the third generations of squarks and from the data on the h^0 mass and coupling κ_b. The fourth column shows constraints at 95% CL obtained by combining the experimental error quadratically with the theoretical uncertainty, except for $B(K_L^0 \to \pi^0 \nu \bar{\nu})$, m_{h^0} and κ_b.

Observable	Exp. data	Theor. uncertainty	Constr. (95%CL)
$10^3 \times \lvert \epsilon_K \rvert$	2.228 ± 0.011 (68% CL) [28]	± 0.28 (68% CL) [29]	2.228 ± 0.549
$10^{15} \times \Delta M_K$ [GeV]	3.484 ± 0.006 (68% CL) [28]	± 1.2 (68% CL) [29]	3.484 ± 2.352
$10^9 \times \text{B}(K_L^0 \to \pi^0 \nu \bar{\nu})$	< 3.0 (90% CL) [28]	± 0.002 (68% CL) [28]	< 3.0 (90% CL)
$10^{10} \times \text{B}(K^+ \to \pi^+ \nu \bar{\nu})$	1.7 ± 1.1 (68% CL) [28]	± 0.04 (68% CL) [28]	$1.7^{+2.16}_{-1.70}$
ΔM_{B_s} [ps^{-1}]	17.757 ± 0.021 (68% CL) [30]	± 2.7 (68% CL) [31]	17.757 ± 5.29
$10^4 \times \text{B}(b \to s\gamma)$	3.49 ± 0.19 (68% CL) [14, 30]	± 0.23 (68% CL) [32]	3.49 ± 0.58
$10^6 \times \text{B}(b \to s\, l^+ l^-)$	$1.60^{+0.48}_{-0.45}$ (68% CL) [33]	± 0.11 (68% CL) [34]	$1.60^{+0.97}_{-0.91}$
$(l = e$ or $\mu)$			
$10^9 \times \text{B}(B_s \to \mu^+ \mu^-)$	$2.8^{+0.7}_{-0.6}$ (68%CL) [35]	± 0.23 (68% CL) [36]	$2.80^{+1.44}_{-1.26}$
$10^4 \times \text{B}(B^+ \to \tau^+ \nu)$	1.14 ± 0.27 (68%CL) [37, 38]	± 0.29 (68% CL) [39]	1.14 ± 0.78
m_{h^0} [GeV]	125.09 ± 0.24 (68% CL) [40]	± 3 [41]	125.09 ± 3.48
κ_b	$1.06^{+0.37}_{-0.35}$ (95% CL) [42]		$1.06^{+0.37}_{-0.35}$ (ATLAS)
	$1.17^{+0.53}_{-0.61}$ (95% CL) [43]		$1.17^{+0.53}_{-0.61}$ (CMS)

- The LHC limits on sparticle masses (at 95% CL) [44]- [48]:

  In the context of simplified models, gluino masses $m_{\tilde{g}} \lesssim 2.1$ TeV are excluded at 95% CL. The mass limit varies in the range 1800-2100 GeV depending on assumptions. First and second generation squark masses are excluded below 1500 GeV. Bottom squark masses are excluded below 1250 GeV. A typical top-squark mass lower limit is ~ 1100 GeV for $m_{\tilde{\chi}_1^0} < 500$ GeV. There is no top-squark mass limit for $m_{\tilde{\chi}_1^0} > 500$ GeV. For sleptons heavier than the lighter chargino $\tilde{\chi}_1^\pm$ and the second neutralino $\tilde{\chi}_2^0$, the mass limits are $m_{\tilde{\chi}_1^\pm}, m_{\tilde{\chi}_2^0} > 650$ GeV for $m_{\tilde{\chi}_1^0} \lesssim 300$ GeV and there is no $m_{\tilde{\chi}_1^\pm}, m_{\tilde{\chi}_2^0}$ limits for $m_{\tilde{\chi}_1^0} > 300$ GeV; For sleptons lighter than $\tilde{\chi}_1^\pm$ and $\tilde{\chi}_2^0$, the mass limits are $m_{\tilde{\chi}_1^\pm}, m_{\tilde{\chi}_2^0} > 1150$ GeV for $m_{\tilde{\chi}_1^0} \lesssim 700$ GeV and there is no $m_{\tilde{\chi}_1^\pm}, m_{\tilde{\chi}_2^0}$ limits for $m_{\tilde{\chi}_1^0} > 700$ GeV.

- The constraint on $(m_{A^0, H^+}, \tan\beta)$ (at 95% CL) from searches for the MSSM Higgs bosons H^0, A^0 and H^+ at LHC, [44, 49–51], where H^0 is the heavier CP-even Higgs boson.

References

[1] G. Aad *et al.* [ATLAS Collaboration], Phys. Lett. B 716 (2012) 1 [arXiv:1207.7214 [hep-ex]].

[2] S. Chatrchyan *et al.* [CMS Collaboration], Phys. Lett. B 716 (2012) 30 [arXiv:1207.7235 [hep-ex]].

[3] S. Heinemeyer *et al.* [LHC Higgs Cross Section Working Group Collaboration], arXiv:1307.1347 [hep-ph].

[4] A. Djouadi, Phys. Rept. **457** (2008) 1 [arXiv:hep-ph/0503172].

[5] A. Bartl, H. Eberl, E. Ginina, K. Hidaka and W. Majerotto, Phys. Rev. D 91 (2015) 015007 [arXiv:1411.2840 [hep-ph]].

[6] H. Eberl, E. Ginina, A. Bartl, K. Hidaka and W. Majerotto JHEP 1606 (2016) 143 [arXiv:1604.02366 [hep-ph]].

[7] For the QCD corrections to $h^0 \to gg$, see K. G. Chetyrkin, B. A. Kniehl, and M. Steinhauser, Nucl. Phys. B 510 (1998) 61 [arXiv:hep-ph/9708255]; M. Kramer, E. Laenen, and M. Spira, Nucl. Phys. B511, 523 (1998), [arXiv:hep-ph/9611272]; Y. Schroder and M. Steinhauser, JHEP 01 (2006) 051 , [arXiv:hep-ph/0512058]; K. G. Chetyrkin, J. H. Kuhn, and C. Sturm, Nucl. Phys. B744 (2006) 121, [arXiv:hep-ph/0512060]; P. A. Baikov and K. G. Chetyrkin, Phys. Rev. Lett. 97 (2006) 061803, [arXiv:hep-ph/0604194]; T. Inami, T. Kubota, and Y. Okada, Z. Phys. C18 (1983) 69; A. Djouadi, M. Spira, and P. M. Zerwas, Phys. Lett. B264 (1991) 440; K. G. Chetyrkin, B. A. Kniehl, and M. Steinhauser, Phys. Rev. Lett. 79 (1997) 353 [arXiv:hep-ph/9705240]; C. Anastasiou, C. Duhr, F. Dulat, F. Herzog, and B. Mistlberger, Phys. Rev. Lett. 114 (2015) 212001 [arXiv:1503.06056[hep-ph]]; M. Schreck and M. Steinhauser, Phys. Lett. B655, 148 (2007) [arXiv:0708.0916 [hep-ph]].

For the QCD corrections to $h^0 \to \gamma\gamma$, see A. Djouadi, M. Spira, and P. M. Zerwas, Phys. Lett. B311 (1993) 255, [arXiv:hep-ph/9305335]; H.-Q. Zheng and D.-D. Wu, Phys. Rev. D42 (1990) 3760; A. Djouadi, M. Spira, J. J. van der Bij, and P. M. Zerwas, Phys. Lett. B257 (1991) 187; S. Dawson and R. P. Kauffman, Phys. Rev. D47 (1993) 1264; K. Melnikov and O. I. Yakovlev, Phys. Lett. B312 (1993) 179 [arXiv:hep-ph/9302281]; M. Inoue, R. Najima, T. Oka, and J. Saito, Mod. Phys. Lett. A9 (1994) 1189; J.Fleischer,O.V.Tarasov,andV.O.Tarasov, Phys. Lett. B584 (2004) 294 [arXiv:hep-ph/0401090]; P. Maierhöfer and P. Marquard, Phys. Lett. B721 (2013) 131 [arXiv:1212.6233 [hep-ph]].

[8] U. Aglietti, R. Bonciani, G. Degrassi, and A. Vicini, Phys. Lett. B595 (2004) 432, [arXiv:hep-ph/0404071]; U. Aglietti, R. Bonciani, G. Degrassi, and A. Vicini, Phys. Lett. B600 (2004) 57, [arXiv:hep-ph/0407162]; S. Actis, G. Passarino, C.

Sturm, and S. Uccirati, Nucl. Phys. B811 (2009) 182, [arXiv:0809.3667[hep-ph]]; G. Degrassi and F. Maltoni, Phys. Lett. B600 (2004) 255, [arXiv:hep-ph/0407249]; S. Actis, G. Passarino, C. Sturm, and S. Uccirati, Phys. Lett. B670 (2008) 12, [arXiv:0809.1301[hep-ph]]; G. Degrassi and F. Maltoni, Nucl. Phys. B724 (2005) 183, [arXiv:hep-ph/0504137].

[9] A. Brignole, Nucl. Phys. B 898 (2015) 644 [arXiv:1504.03273 [hep-ph]].

[10] M. Spira, A. Djouadi, D. Graudenz and P. M. Zerwas, Nucl. Phys. B 453 (1995) 17 [arXiv:hep-ph/9504378].

[11] M. Endo, T. Moroi, M. Nojiri, JHEP 04 (2015) 176 [arXiv:1502.03959 [hep-ph]]; S. Boselli, R. Hunter and A. Mitov, arXiv:1805.12027 [hep-ph].

[12] B. C. Allanach *et al.*, Comput. Phys. Commun. **180** (2009) 8 [arXiv:0801.0045 [hep-ph]].

[13] F. Gabbiani, E. Gabrielli, A. Masiero and L. Silvestrini, Nucl. Phys. B 477 (1996) 321 [arXiv:hep-ph/9604387].

[14] C. Patrignani et al. (Particle Data Group), Chin. Phys. C, 40, 100001 (2016).

[15] A. Dedes et al., JHEP 2014 (2014) 137 [arXiv:1409.6546 [hep-ph]].

[16] W. Porod, Comput. Phys. Commun. **153** (2003) 275 [arXiv:hep-ph/0301101].

[17] W. Porod and F. Staub, Comput. Phys. Commun. **183** (2012) 2458 [arXiv:1104.1573 [hep-ph]].

[18] D. M. Pierce et al., Nucl. Phys. B 491 (1997) 3.

[19] L. G. Almeida, S. J. Lee, S. Pokorski and J. D. Wells, Phys. Rev. D 89 (2014) no.3, 033006 [arXiv:1311.6721v3 [hep-ph]].

[20] LHC Higgs Cross Section Working Group, D. de Florian, C. Grojean, F. Maltoni, C. Mariotti, A. Nikitenko, M. Pieri, P. Savard, M. Schumacher, R. Tanaka (Eds.), Handbook of LHC Higgs Cross Sections: 4. Deciphering the nature of the Higgs sector, CERN Yellow Reports: Monographs, Vol. 2/2017, CERN-2017-002-M (CERN, Geneva, 2017), https://doi.org/10.23731/CYRM-2017-002, [arXiv:1610.07922].

[21] K. Fujii et al., arXiv:1710.07621.

[22] H. Abramowicz et al., arXiv:1307.5288[hep-ex].

[23] ATLAS collaboration, ATLAS-CONF-2018-031.

[24] CMS collaboration, CMS-HIG-16-040, CERN-EP-2018-060 [arXiv:1804.02716].

[25] J. Tian, email correspondence.

[26] H. Eberl, E. Ginina, K. Hidaka, Euro Physical Journal C77 (2017) 189 [arXiv:1702.00348 [hep-ph]].

[27] W. Peng et al., Phys. Lett. B618 (2005) 209 [arXiv:hep-ph/0505086 [hep-ph]]; S. Dittmaier et al., Phys. Rev. D90 (2014) 035010 [arXiv:1406.5307 [hep-ph]].

[28] M. Tanabashi et al. (Particle Data Group), Phys. Rev. D 98 (2018) 030001 and 2019 update.

[29] J. Brod and M. Gorbahn, Phys. Rev. Lett. 108 (2012) 121801 [arXiv:1108.2036 [hep-ph]].

[30] Y. Amhis et al. (Heavy Flavour Averaging Group), "Averages of b-hadron, c-hadron, and tau-lepton properties as of summer 2016", arXiv:1612.07233[hep-ex].

[31] T. Jubb, M. Kirk, A. Lenz, and G. Tetlalmatzi-Xolocotzi, arXiv:1603.07770 [hep-ph]; M. Artuso, G. Borissov, and A. Lenz, Rev. Mod. Phys. 88 (2016) 045002 [arXiv:1511.09466 [hep-ph]].

[32] M. Misiak et al., Phys. Rev. Lett. 114 (2015) 221801 [arXiv:1503.01789[hep-ph]].

[33] J.P. Lees *et al.* [BABAR Collaboration], Phys. Rev. Lett. 112 (2014) 211802 [arXiv:1312.5364 [hep-ex]].

[34] T. Huber, T. Hurth and E. Lunghi, Nucl. Phys. B 802 (2008) 40 [arXiv:0712.3009 [hep-ph]].

[35] V. Khachatryan et al. [CMS and LHCb Collaborations], Nature 522 (2015) 68 [arXiv:1411.4413[hep-ex]].

[36] C. Bobeth *et al.*, Phys. Rev. Lett. 112 (2014) 101801 [arXiv:1311.0903 [hep-ph]].

[37] K. Trabelsi, plenary talk at European Physical Society Conference on High Energy Physics 2015 (EPS-HEP2015), Vienna, 22 - 29 July 2015.

[38] P. Hamer, talk at European Physical Society Conference on High Energy Physics 2015 (EPS-HEP2015), Vienna, 22 - 29 July 2015.

[39] J. M. Roney, talk at 26th International Symposium on Lepton Photon Interactions at High Energies, San Francisco, USA, 24-29 June 2013.

[40] ATLAS and CMS collaborations, Phys. Rev. Lett. 114 (2015) 191803, [arXiv:1503.07589[hep-ex]].

[41] S. Borowka, T. Hahn, S. Heinemeyer, G. Heinrich and W. Hollik, Eur. Phys. J. C75 (2015) 424 [arXiv:1505.03133 [hep-ph]].

[42] H. M. Gray, talk at 54th Rencontres de Moriond on Electroweak Interactions and Unified Theories, La Thuile, Italy, 16 - 23 Mar 2019 [ATLAS Collaboration, ATLAS-CONF-2019-005].

[43] CMS Collaboration, Eur. Phys. J. C 79 (2019) 421 [arXiv:1809.10733 [hep-ex]].

[44] M. D'Onofrio, plenary talk at EPS Conference on High Energy Physics (EPS-HEP2017), Venice, Italy, 5-12 July 2017.

[45] E. Kuwertz, talk at 52nd Rencontres de Moriond EW 2017, La Thuile, 18-25 March, 2017; ATLAS Collaboration, ATLAS-CONF-2017-022 (submitted to 52nd Rencontres de Moriond on Electroweak Interactions and Unified Theories, La Thuile, Italy, 18 - 25 Mar 2017); A. Petridis, talk at 52nd Rencontres de Moriond on Electroweak Interactions and Unified Theories, La Thuile, Italy, 18 - 25 Mar 2017.

[46] ATLAS Collaboration, JHEP 05 (2014) 071 [arXiv:1403.5294[hep-ex]]; CMS Collaboration, EPJC 74 (2014) 3036 [arXiv:1405.7570[hep-ex]].

[47] M. Marionneau, talk at 52nd Rencontres de Moriond on Electroweak Interactions and Unified Theories, La Thuile, Italy, 18 - 25 Mar 2017.

[48] S. Strandberg, plenary talk at XXXIX International Conference on High Energy Physics, July 4-11, 2018, Seoul.

[49] D. Charlton, plenary talk at 38th International Conference on High Energy Physics (ICHEP2016), Chicago, 3 - 10 August 2016.

[50] C. Gwilliam, talk at 38th International Conference on High Energy Physics (ICHEP2016), Chicago, 3 - 10 August 2016; ATLAS Collaboration, ATLAS-CONF-2016-088.

[51] D. N. Taylor, talk at 54th Rencontres de Moriond on Electroweak Interactions and Unified Theories, La Thuile, Italy, 16 - 23 Mar 2019; CMS Collaboration, JHEP 1809 (2018) 007 [arXiv:1803.06553 [hep-ex]].

[52] M. Tanabashi et al. (Particle Data Group), Phys. Rev. D 98, 030001 (2018).